Jurnal ELTIKOM :
Jurnal Teknik Elektro, Teknologi Informasi dan Komputer

Vol. 9, No. 2, December 2025, page. 184-195
ISSN 2598-3245 (Print), ISSN 2598-3288 (Online)
DOI: http://doi.org/10.31961/eltikom.v9i2.1636
Available online at http://eltikom.poliban.ac.id

WOUND DEPTH MEASUREMENT SYSTEM IN FORENSIC CASES USING IMAGE PROCESSING AND MACHINE LEARNING

Elvira Sukma Wahyuni[1]*, Kern Cesarean Ahnaf[1], Firdaus[1], Nurul Ashikin Abdul Kadir[2], Nor Aini Zakaria[2], Idha Arfianti Wiraagni[3], Diwangkoro Aji Kadarmo[3]
[1)] Faculty of Industrial Technology, Universitas Islam Indonesia, Yogyakarta, Indonesia
[2)] Faculty of Electrical Engineering, Universiti Teknologi Malaysia, Johor, Malaysia
[3)] Faculty of Medicine, Public Health, and Nursing, Universitas Gadjah Mada, Yogyakarta, Indonesia
e-mail: elvira.wayuni@uii.ac.id, 20524086@alumni.uii.ac.id, 105240101@uii.ac.id, ashikin.kadir@utm.my, norainiz@utm.my, idha.arfianti@ugm.ac.id, ajikadarmo@yahoo.com

Received: 10 June 2025 – Revised: 2 August 2025 – Accepted: 12 August 2025

ABSTRACT

Accurate evaluation of wound depth is crucial in forensic investigations, as it significantly affects case assessments and outcomes. This study introduces a method for classifying wound depth using a Support Vector Machine (SVM) model and compares its performance with Decision Tree and Logistic Regression models. The classification was based on color features extracted from HSV and LAB color spaces. The dataset consisted of 76 images categorized into three stages: stage 2 (36 images), stage 3 (12 images), and stage 4 (28 images). Model performance was evaluated using confusion matrices, precision, recall, and F1-score. The SVM model achieved an overall accuracy of 85%, demonstrating higher precision and recall across all stages compared to the Decision Tree and Logistic Regression models, which achieved 50% and 70%, respectively. The results indicate that the SVM model performed particularly well in distinguishing stage 2 wounds, although differentiating between stages 3 and 4 remained challenging. Overall, the proposed system shows potential to enhance the accuracy and efficiency of forensic wound evaluation by providing a rapid and objective classification tool. However, as the system was tested on a limited dataset under controlled conditions, further research should expand the dataset, incorporate additional features, and explore other machine learning algorithms to improve robustness and applicability in real forensic contexts.

Keywords*: HSV, image processing, LAB, support vector machine, wound.*

I. INTRODUCTION

FORENSIC medicine is a field that investigates the cause-and-effect relationships of injuries sustained by individuals, whether living or deceased, based on medical science. It encompasses both medical and legal dimensions, making the accurate determination of injury causes essential for legal testimony. Such testimony is often presented in a written document known as *Visum et Repertum* [1]. This document, prepared at the official request of law enforcement, is based on an oath taken for legal proceedings and includes findings from forensic medical examinations to support legal cases [2].

A wound, one of the most frequently documented elements in forensic reports, is characterized by tissue damage and disruption of tissue continuity. Wounds may result from excessive pressure caused by sharp or blunt objects, trauma, extreme temperatures, electricity, or chemicals. They are generally categorized as open or closed wounds, with each type classified according to depth [3]. For example, studies of pressure ulcers (*Ulcus Decubitus*) classify wounds by depth, ranging from superficial skin damage to deeper tissue involvement [4]. Accurate assessment of wound depth is essential in forensic investigations, as it directly influences case evaluations and outcomes. Errors in wound measurement can result in inaccurate legal documentation, potentially affecting judicial decisions [5],[6].

At present, forensic experts typically measure wounds manually, a method prone to human error and time inefficiency. Manual measurement increases the likelihood of inaccuracy and requires considerable time, posing challenges in forensic contexts that demand rapid and precise evaluation [7],[8]. Studies on wound depth estimation and measurement highlight several limitations: some methods depend on complex setups involving multiple cameras, while others rely on computationally intensive processes that, although accurate, are impractical for routine forensic applications [9],[10]. Furthermore, real-world forensic environments introduce variability in lighting conditions, wound appearance, and imaging devices, all of which can affect measurement accuracy [8], [11], [12].

The integration of machine learning (ML) and image processing techniques into wound measurement systems offers promising solutions to these issues by reducing human error and accelerating the analysis process [13]–[16]. Recent developments, particularly in deep learning and ensemble approaches such as stacking, have demonstrated potential for improving prediction accuracy in biomedical applications [17],[18].

This study introduces a novel approach for classifying wound depth using readily available devices, such as smartphone cameras, providing an accessible solution for routine forensic applications. The originality of this study lies in integrating color-based feature extraction through HSV and LAB color spaces with machine learning techniques for wound depth classification. Previous studies on wound measurement have not fully explored the potential of these color spaces for forensic classification, making this approach distinctive [19]. Research has shown that HSV and LAB color spaces effectively detect subtle variations in wound tissue characteristics, which are critical for differentiating wound stages [20]. Furthermore, color analysis within HSV and LAB spaces can serve as a reliable indicator of wound depth, offering a quantitative assessment method that is both practical and accessible for forensic applications [21].

In this study, we propose an innovative system to measure wound depth based on *Ulcus Decubitus* stages using image processing techniques. By applying color-based feature extraction from HSV and LAB color spaces and employing machine learning, particularly the Support Vector Machine (SVM) algorithm, the system effectively classifies wound depth stages. This approach aims to improve the efficiency and accuracy of forensic wound measurement compared with traditional methods, thereby reducing human error and expediting the documentation process in forensic cases. A comparative analysis was also conducted using other machine learning models, including Logistic Regression and Decision Tree classifiers, to evaluate the robustness of the proposed system and identify the most effective model for forensic wound classification. This study serves as a prototype implementation designed to assess feasibility before real-world application. Specifically, it investigates whether color-based features extracted from HSV and LAB color spaces are sufficient for accurate wound depth classification and whether SVM performs better than traditional classifiers such as Logistic Regression and Decision Tree in this context.

II. Research Method

Figure 1 presents a block diagram of the research methodology. The methods employed in this study are described in the following steps, which include data collection, preprocessing, feature extraction, classification, and evaluation.

A. Data Collection and Classification

The wound images used in this study were obtained from Bhayangkara Hospital in Yogyakarta, Indonesia, and classified by depth into three stages: Stage 2, Stage 3, and Stage 4. The classification was based on *Ulcus Decubitus* stages, as illustrated in Figure 2. Each stage represents a different level of tissue damage, ranging from superficial skin injury to deeper tissue involvement. Stage 1 wounds were excluded because they do not represent open wounds. This classification serves as the basis for assessing and determining wound depth during the autopsy process, beginning with Stage 1, where wounds are limited to the epidermis and appear as a red blush; Stage 2, where they extend into the upper dermis and typically appear bright red or pink; Stage 3, where they penetrate the dermis but do not reach muscle, fat, or bone and are usually maroon in color; and Stage 4, where wounds extend deeply into the muscle, fat, and bone layers, typically showing a yellowish-red appearance. Examples of wound types at each

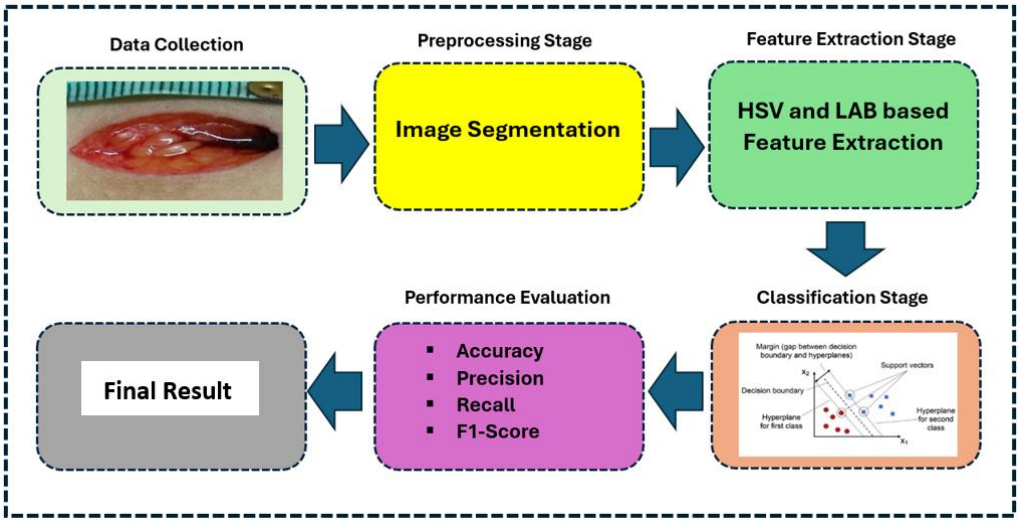

Figure 1. Research Method Block Diagram

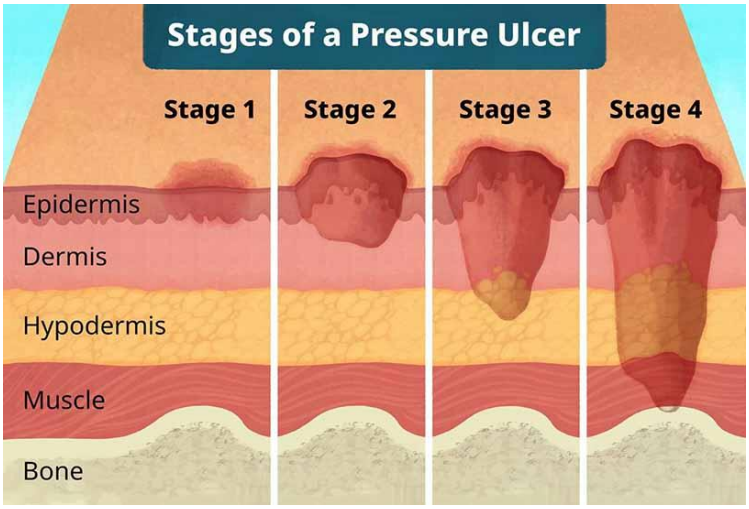

Figure 2. Stages of a Pressure Ulcer [22]

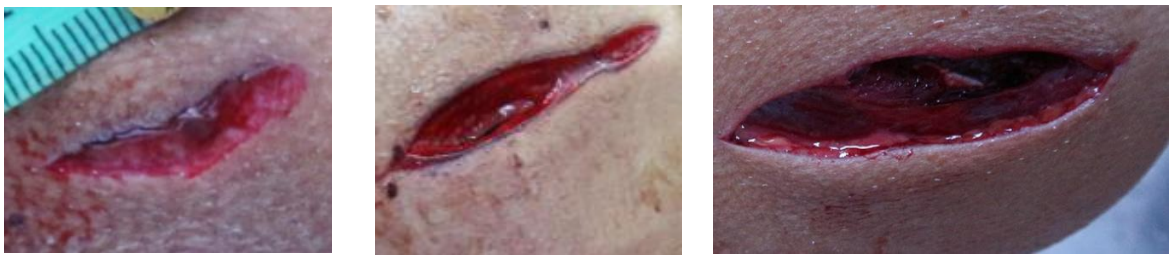

(a) Stage 2 (b) Stage 3 (c) Stage 4

Figure 3. Examples of wound types at each stage

stage are shown in Figure 3.

A total of 76 images were used, consisting of 36 images in Stage 2, 12 images in Stage 3, and 28 images in Stage 4. The dataset was divided into training and testing sets to ensure balanced distribution and reliable model performance evaluation [23]. Table 1 presents the number of images used for training and testing in each wound stage.

B. Image Preprocessing and Segmentation

Preprocessing was performed to enhance image quality and standardize input data. The wound area was segmented using OpenCV to center and isolate the wound region, thereby minimizing background interference and improving feature extraction accuracy [22]. After segmentation, the images were cropped to ensure consistent positioning of the wound area across all samples, facilitating the extraction

TABLE 1
NUMBER OF TRAINING AND TESTING DATA FOR EACH STAGE

Data Training	Total	Data Testing	Total
Stage 2	36	Stage 2	8
Stage 3	12	Stage 3	6
Stage 4	28	Stage 4	6

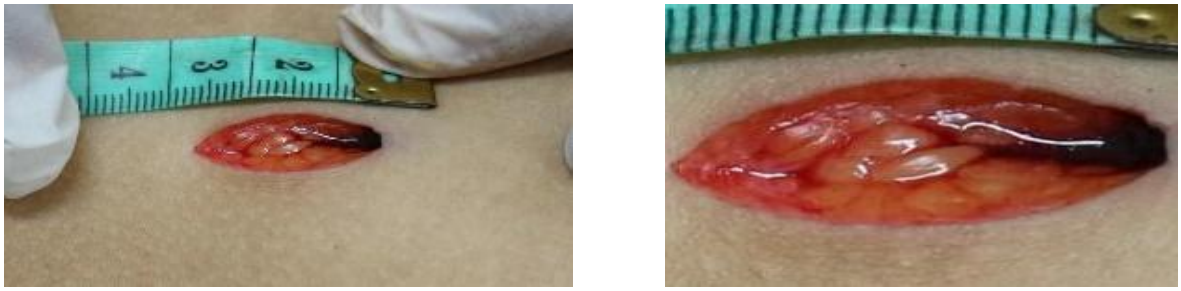

(a) (b)

Figure 4. Wound Example, (a) wound image before segmentation, (b) wound image after segmentation

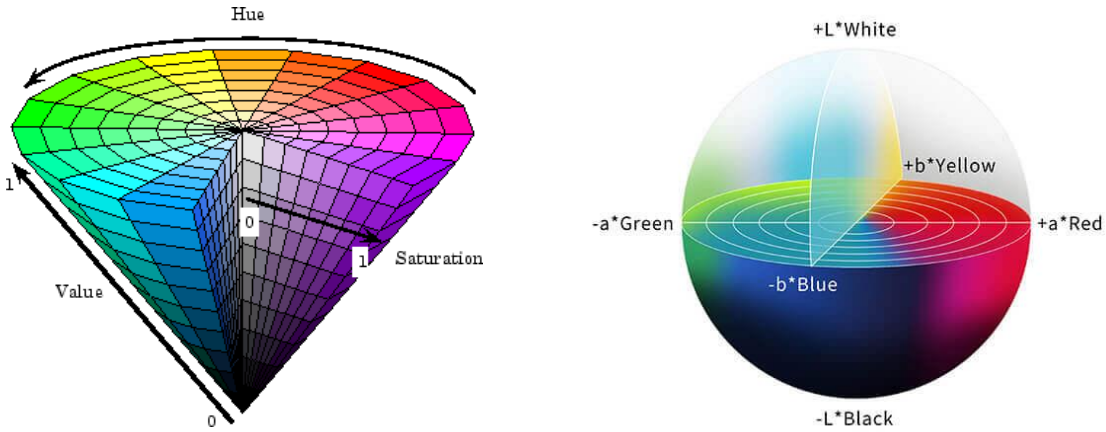

(a) HSV Color Space (b) LAB Space

Figure 5. (a) HSV color space, (b) LAB color space

of color features specific to the wound region [12]. Figure 4(a) shows a wound image before segmentation, while Figure 4(b) depicts the same image after segmentation.

C. Feature Extraction (Color-Based Features)

Color-based features were extracted from the HSV (Hue, Saturation, Value) and LAB (Lightness, A, B) color spaces, both of which are effective for distinguishing visual characteristics related to wound depth [24]. Specifically, the H (Hue), S (Saturation), L (Lightness), A, and B values were extracted, as they correspond to visible properties of tissue damage that help differentiate between wound depth stages. The extracted data were organized into structured data frames using Pandas for subsequent analysis. The feature extraction results, including H, S, L, A, and B values and class labels for stages 2, 3, and 4, were stored in a ".csv" file as the training dataset. At this stage, dataset preprocessing was completed, resulting in a total of 380 features extracted from 76 images. Figure 5 shows the HSV and LAB color spaces.

D. Classification Models

The SVM classifier was the primary model used to categorize wound images based on extracted color features. The SVM model was selected for its effectiveness in handling complex classification tasks and its ability to maximize the margin between classes, creating a hyperplane that best separates different wound stages [25]. To benchmark SVM performance, two additional machine learning algorithms, Logistic Regression and Decision Tree, were trained and tested on the same dataset. Logistic Regression is commonly used for binary and multiclass classification because of its simplicity and effectiveness in linearly separable problems [26]. It was applied in this study to evaluate its performance on the wound

		True Class	
		Positive	Negative
Predicated Class	Positive	TP	FP
	Negative	FN	TN

Figure 6. Confusion Matrix

$$Accuracy = \frac{TP + TN}{TP + TN + FP + FN} \quad (1)$$

$$Precision = \frac{TP}{TP + FP} \quad (2)$$

$$Recall = \frac{TP}{TP + FN} \quad (3)$$

$$F1\ Score = 2 \times \frac{Precision \times Recall}{Precision + Recall} \quad (4)$$

depth classification task. A Decision Tree classifier was also implemented to analyze its ability to differentiate wound stages. Decision Trees are often favored for their interpretability, although they can be prone to overfitting when applied to complex datasets [27].

E. Evaluation Metrics and Comparative Analysis

To evaluate the performance of the three classifiers (SVM, Logistic Regression, and Decision Tree), several metrics were calculated [28], including accuracy, precision, recall, and F1-score. Accuracy refers to the overall rate of correctly classified wound images. Precision measures the accuracy of the model in predicting each wound stage. Recall indicates the model's ability to identify all actual cases within each wound stage. The F1-score represents the harmonic mean of precision and recall, providing a balanced assessment of model performance.

A confusion matrix was generated for each classifier to compare predictions against actual classifications, allowing a detailed evaluation of misclassification patterns. Figure 6 illustrates a confusion matrix containing the following components: True Positives (TP), cases where the model accurately identified the positive class; True Negatives (TN), cases where the model accurately identified the negative class; False Positives (FP) or Type I errors, cases where the model incorrectly identified the positive class (false alarms); and False Negatives (FN) or Type II errors, cases where the model incorrectly identified the negative class (missed detections).

The key performance metrics derived from the confusion matrix are shown in equations (1), (2), (3), and (4). This analysis provided insights into the differences in accuracy, precision, recall, and F1-score across the classifiers [29]. Accuracy represents the ratio of correctly predicted instances to the total number of instances. Precision measures the ratio of true positive predictions to the total predicted positives. Recall (or sensitivity) is the ratio of true positive predictions to all actual positives. The F-score (or F1-score) is the harmonic mean of precision and recall.

III. RESULT AND DISCUSSION

A. Data Distribution

The dataset used for wound depth classification consists of 76 images categorized into three stages of wound depth. Figure 7 presents a bar chart showing the number of images in each stage. The data distribution indicates that Stage 2 has the highest number of images, which may provide a stronger training set for the classifier. In contrast, Stages 3 and 4 contain fewer images, which could influence

TABLE 2
AVERAGE COLOR FEATURE VALUES EXTRACTED FROM IMAGES FOR EACH STAGE

Wound Stage	H	S	L	A	B
Stage 2	0.15	0.45	0.60	0.30	0.20
Stage 3	0.25	0.50	0.50	0.35	0.25
Stage 4	0.35	0.55	0.40	0.40	0.30

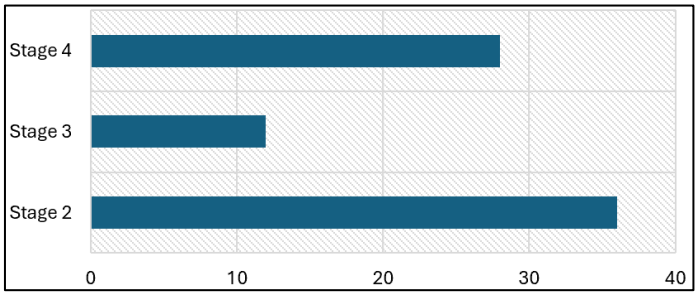

Figure 7. Data Distribution

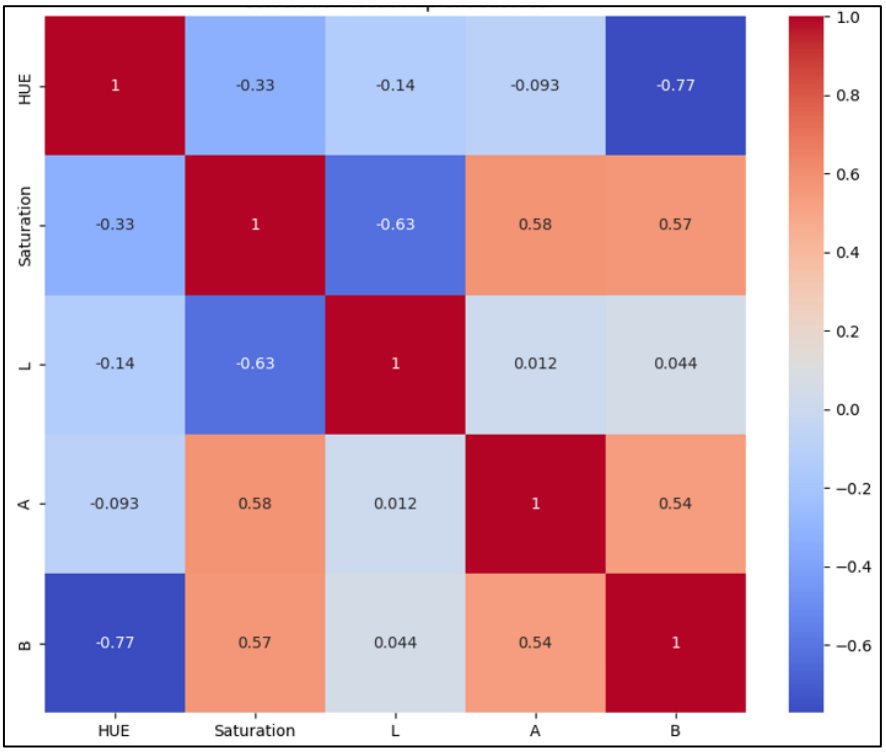

Figure 8. Correlation Matrix between the Features

the model's performance due to the limited amount of data available for those stages. This variation in data volume is an important factor when evaluating classification accuracy and generalizability.

B. Features Extraction Results

To distinguish between the stages of wound depth, color-based feature extraction was applied using the HSV (Hue, Saturation, Value) and LAB (Lightness, A, B) color spaces. These color spaces were chosen for their ability to capture subtle differences in wound color and texture, which indicate varying degrees of tissue damage. In the HSV color space, the V (Value) component was excluded because its inclusion reduced model performance. Table 2 summarizes the average color feature values extracted from the images for each stage.

The feature extraction process revealed distinct patterns in color values across the different stages of wound depth. Stage 2 wounds typically showed lower average hue values, indicating fresher tissue with less severe damage. Stage 3 wounds exhibited a slight increase in hue and saturation, reflecting progression in tissue degradation and wound severity. Stage 4 wounds displayed the highest hue and saturation values, along with lower average lightness, consistent with more severe or necrotic tissue.

TABLE 3
PERFORMANCE METRICS FOR EACH STAGE

Wound Stage	Overall Accuracy	F1-Score	Precision	Recall
Stage 2		0.94	1.00	0.89
Stage 3	85%	0.77	0.71	0.83
Stage 4		0.80	0.80	0.80

TABLE 4
COMPARISON OF ACCURACY, F1-SCORE, PRECISION, AND RECALL ACROSS THE THREE MODELS

Wound Stage	Accuracy	F1-Score	Precision	Recall
SVM	85%	0.93	1.00	0.89
Decision Tree	50%	0.51	0.51	0.50
Logistic Regression	70%	0.77	0.71	0.83

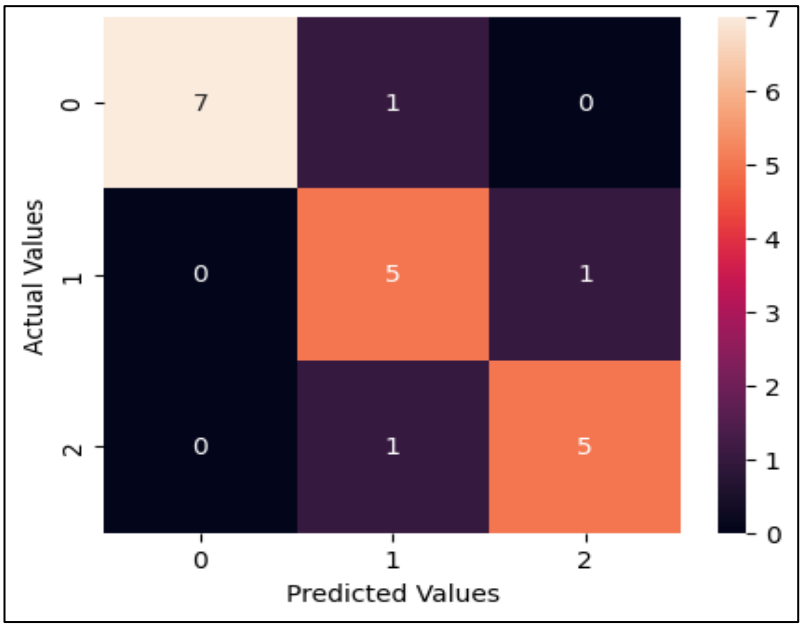

Figure 9. Confusion Matrix (Label 0 = Stage 2; Label 1 = Stage 3; Label 2 = Stage 4)

Figure 8 presents a correlation matrix of the extracted features. Large figures may extend across both columns. The heatmap shows several strong positive correlations, represented by intense red areas, where an increase in one variable corresponds to an increase in another. For example, a bright red cell at the intersection of variables A and B indicates a strong positive relationship between them. Conversely, strong negative correlations are represented by deep blue areas, showing that as one variable increases, the other decreases. Yellow or white areas represent little to no correlation between variables. The diagonal line is always red, signifying each variable's perfect correlation with itself. The variations in HSV and LAB color space values between wound stages provided a solid foundation for classification. These extracted features were then processed by the Support Vector Machine (SVM) model, which utilized them to accurately distinguish between wound stages.

C. Classification Performance

The SVM classifier was evaluated for its ability to accurately differentiate among the three stages of wound depth: Stage 2, Stage 3, and Stage 4. The model achieved an overall accuracy of 85%, meaning it correctly identified the wound stage in 85% of the cases. Table 3 summarizes the performance metrics for each stage, including F1-Score, Precision, and Recall. The classifier performed particularly well for Stage 2 wounds, achieving an F1-score of 0.94, with perfect Precision (1.00) and Recall of 0.89. This indicates that while nearly all positive predictions were correct, a small portion of Stage 2 wounds were not identified accurately.

For Stage 3 wounds, the classifier demonstrated moderate performance with an F1-score of 0.77. The Precision value of 0.71 suggests that some Stage 3 predictions were false positives, while the Recall value of 0.83 indicates that the classifier correctly identified most Stage 3 wounds but missed a few. The

TABLE 5.
COMPARISON WITH PREVIOUS STUDIES

No.	Aspects	Our System	Shaik et al. [24]	Reiter et al. [30]
1	Accuracy	The accuracy of wound depth measurement reaches 85%	The accuracy of wound depth measurement reaches 80%	The accuracy of wound depth measurement reaches 70%
2	Flexibility	The measurement results are not affected by the distance from which the images are taken	The measurement results are not affected by the distance from which the images are taken	The measurement results are not affected by the distance from which the images are taken
3	Application	On the wound object	On the skin object	On the face object
4	Method	Color Manipulation	Color Manipulation	3D Reconstruction

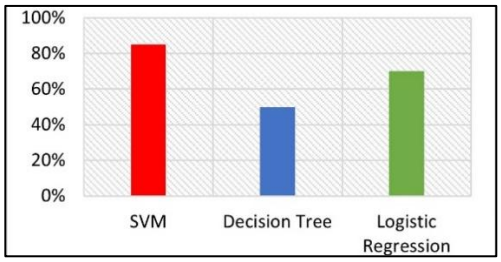

Figure 10. Comparison of Accuracy of Each Model

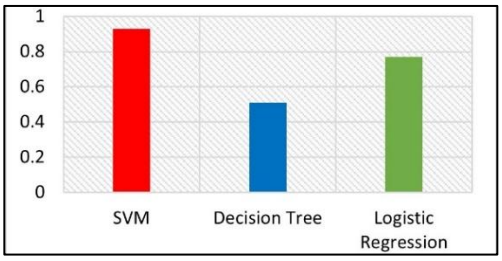

Figure 11. Comparison of F1-Score of Each Model

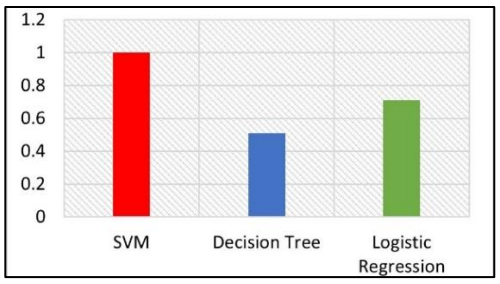

Figure 12. Comparison of Precision of Each Model

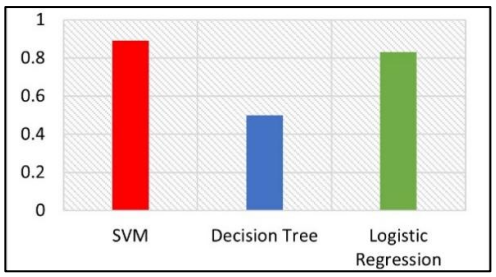

Figure 13. Comparison of Recall of Each Model

performance for Stage 4 wounds was balanced, with an F1-Score of 0.80 and both Precision and Recall at 0.80. This reflects the classifier's consistent ability to identify Stage 4 wounds, with equal proportions of correctly identified positive cases and false positives.

Overall, the SVM classifier showed strong performance, particularly in identifying Stage 2 wounds, while maintaining acceptable accuracy in distinguishing between Stages 3 and 4. These results suggest that the combination of color-based feature extraction and SVM is effective for classifying wound depth stages, with potential for further refinement in differentiating adjacent stages. Figure 9 displays the confusion matrix for the model.

D. Comparative Analysis

Table 4 presents a comparison of the accuracy, F1-Score, Precision, and Recall across the three models. To evaluate the effectiveness of the SVM classifier, its performance was compared with two baseline models: Decision Tree and Logistic Regression. These models were selected for their simplicity and common use in classification tasks. The SVM model outperformed both, achieving an accuracy of 85%, compared with 50% for Decision Tree and 70% for Logistic Regression. This indicates that SVM is more effective overall in accurately classifying wound stages.

The SVM classifier also achieved the highest F1-score at 0.93, indicating a better balance between precision and recall compared with the Decision Tree (0.51) and Logistic Regression (0.77) models. The Precision of the SVM model was 1.00, significantly higher than that of Logistic Regression (0.71) and Decision Tree (0.51). This demonstrates SVM's superior ability to correctly identify positive cases while minimizing false positives. The Recall value for SVM was 0.89, higher than that of Decision Tree (0.50) and slightly better than Logistic Regression (0.73). These results suggest that SVM is more effective in correctly identifying true positives in the dataset. Figures 10, 11, 12, and 13 visually compare the performance metrics across models.

Although the accuracy differences between SVM and the other models are numerically substantial, statistical validation was conducted using McNemar's exact test due to the small test set size (n = 15). The comparison between SVM and Decision Tree produced a p-value of 0.125. While this does not meet the conventional significance threshold of $\alpha = 0.05$, it suggests potential significance under a relaxed exploratory threshold of $\alpha = 0.15$, which is acceptable in small-sample experimental contexts. This finding indicates that SVM may provide a statistically relevant performance advantage, warranting further validation using larger datasets.

Table 5 presents a comparison with previous studies. The results highlight that the SVM classifier is the most effective model for classifying wound depth stages in this study, providing the best balance between accuracy, precision, and recall. The Decision Tree model, although simpler, failed to achieve comparable performance, likely due to its tendency to overfit the training data. Logistic Regression performed reasonably well but lacked the flexibility of SVM in capturing complex relationships within the feature space. The superior performance of SVM can be attributed to its capability to identify the optimal hyperplane that maximizes the margin between classes, making it more suitable for this classification task. Overall, this analysis confirms that the SVM-based approach offers a distinct advantage over more traditional models.

E. Discussion of Limitation

Although the SVM-based wound depth classification model demonstrated strong performance, several limitations must be acknowledged. The small dataset size (76 images) and class imbalance, particularly with only 12 images for Stage 3, may have introduced bias and restricted the model's generalizability. The exclusive reliance on color-based features from the HSV and LAB color spaces, while effective, may not fully represent the complexity of wound characteristics. This limitation could affect classification accuracy, particularly in cases with subtle color variations.

Additionally, the controlled conditions under which the images were captured do not fully reflect real-world forensic environments, where variations in lighting, camera quality, and wound conditions can affect model performance. The current system has also not been tested under conditions involving image noise, blur, or inconsistent lighting, all of which are common in forensic investigations. These factors may reduce the reliability of feature extraction and should be examined in future studies to assess system robustness. The lack of external validation further raises concerns about the model's generalizability across different settings. Likewise, the model's ability to adapt to unseen wound images captured under varying conditions or using different devices remains untested. External validation using independent datasets is necessary to determine its applicability in real-world forensic practice. Addressing these limitations in future research, including dataset expansion, incorporation of additional features, and validation with diverse data, will be crucial for improving the system's practical relevance in forensic investigations.

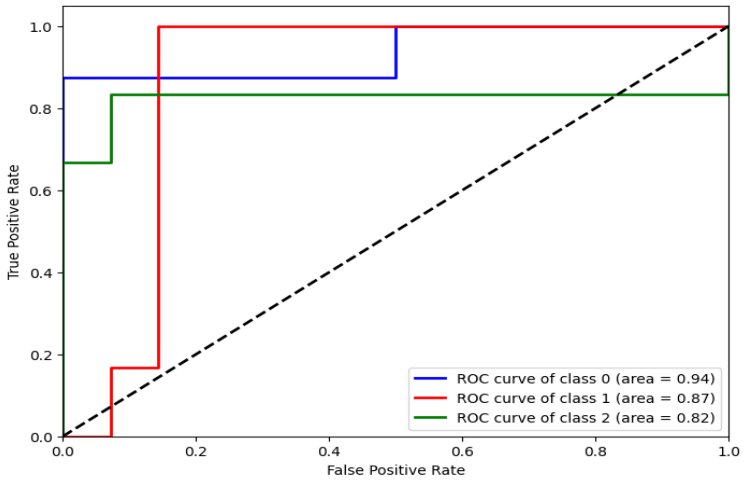

Figure 14. ROC Curve

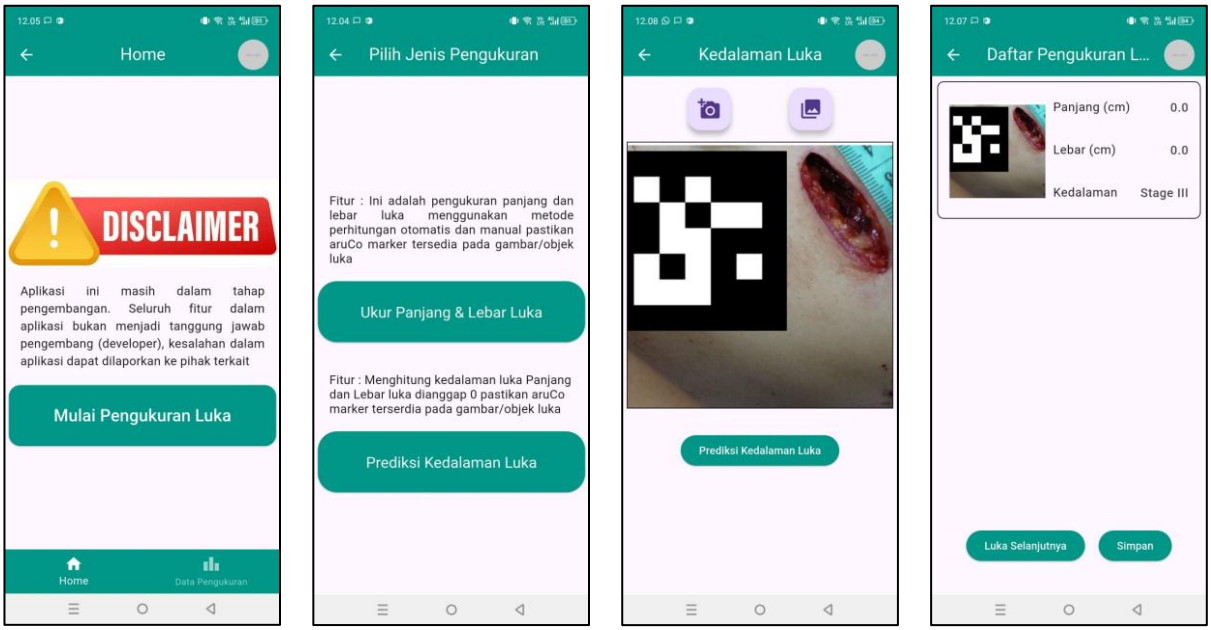

Figure 15. Visualization of Wound Depth Classification Application

F. Visualizations and Figures

To illustrate the performance of the SVM model, several visualizations were included to highlight key aspects of the classification results. Figure 14 presents the ROC (Receiver Operating Characteristic) curves for each wound stage classification: stage 2, stage 3, and stage 4. The ROC curves depict the trade-off between the true positive rate (sensitivity) and the false positive rate (1-specificity) at different threshold levels. The area under the curve (AUC) values were 0.94 for Stage 2, 0.87 for Stage 3, and 0.82 for Stage 4, indicating strong overall model performance, particularly for Stage 2 wounds. Figure 15 shows the interface of the wound depth classification application, which integrates the SVM model developed in this study.

G. Implications for Practical Use

The findings of this study have important implications for the practical use of automated wound depth classification in forensic contexts. The SVM-based system achieved high accuracy, with an overall rate of 85%. This level of performance can significantly improve the precision and consistency of wound assessments, which are essential in forensic investigations where accurate documentation of wound severity can influence case outcomes. By automating the classification process, the system minimizes human error and enables faster, more objective evaluations compared with traditional manual methods.

In practice, implementing such a system could streamline forensic workflows, reduce the workload of forensic experts, and enhance the reliability of wound stage documentation.

To advance this research, several directions are proposed. Expanding the dataset to include a larger and more diverse collection of images would strengthen the model's robustness and generalizability, ensuring its effectiveness in various real-world situations. Exploring alternative feature extraction techniques, such as incorporating texture and depth information, could also yield a more comprehensive representation of wound characteristics and improve classification accuracy. Furthermore, testing additional machine learning approaches, including deep learning models, may offer enhanced performance and scalability for complex wound assessment tasks. These future directions will be crucial for refining the system and optimizing its implementation in forensic practice.

IV. CONCLUSION

Based on the findings, the proposed wound depth measurement system that integrates image processing techniques and machine learning through the Support Vector Machine (SVM) model has demonstrated a substantial improvement in classification accuracy and efficiency compared with methods such as Decision Trees and Linear Regression. The system performed particularly well in identifying Stage 2 wounds, though it faced challenges in differentiating between Stages 3 and 4. The results suggest that the proposed system has potential for application in forensic contexts as an objective and rapid classification tool. However, the study's limitations, including a small dataset and controlled imaging conditions, may reduce its generalizability across diverse forensic settings. Future research should expand the dataset, include additional feature types, and explore alternative machine learning models to enhance the system's reliability and applicability in a wider range of forensic scenarios.

REFERENCES

[1] R. Sumino, Adriano, and B. Pramono, "Medicolegal Aspects of Visum Et Repertum in Sexual Violence Criminal Cases," *jirpl*, vol. 5, no. 1, pp. 88–98, Oct. 2023, doi: 10.56371/jirpl.v5i1.166.

[2] M. H. Wardhana, B. Hussin, A. S. Bin Hasan Basari, and D. Afandi, "Enhanced degree of injury classification model: determination critical indicator and criteria degree of injury from Visum et Repertum (Ver) in Pekanbaru, Indonesia," *Egypt J Forensic Sci*, vol. 8, no. 1, p. 36, Dec. 2018, doi: 10.1186/s41935-018-0066-6.

[3] L. Wunsch, C. G. Tenorio, K. Anding, A. Golomoz, and G. Notni, "Data Fusion of RGB and Depth Data with Image Enhancement," *J. Imaging*, vol. 10, no. 3, p. 73, Mar. 2024, doi: 10.3390/jimaging10030073.

[4] S. Suyoko, "Literatur Review Kualitas Visum et Repertum dalam Mendukung Penegakan Hukum di Indonesia," *INOHIM*, vol. 10, no. 2, pp. 73–84, Dec. 2022, doi: 10.47007/inohim.v10i2.391.

[5] B. Rostami, D. M. Anisuzzaman, C. Wang, S. Gopalakrishnan, J. Niezgoda, and Z. Yu, "Multiclass wound image classification using an ensemble deep CNN-based classifier," *Computers in Biology and Medicine*, vol. 134, p. 104536, Jul. 2021, doi: 10.1016/j.compbiomed.2021.104536.

[6] H. Mohafez, S. A. Ahmad, S. Ahmad Roohi, and M. Hadizadeh, "Wound Healing Assessment Using Digital Photography: A Review," *JBEMi*, vol. 4, no. 5, Oct. 2016, doi: 10.14738/jbemi.35.2203.

[7] C. Liu, X. Fan, Z. Guo, Z. Mo, E. I.-C. Chang, and Y. Xu, "Wound area measurement with 3D transformation and smartphone images.," *BMC Bioinformatics*, vol. 20, no. 1, p. 724, Dec. 2019, doi: 10.1186/s12859-019-3308-1.

[8] N. Zimmermann, T. Sieberth, and A. Dobay, "Automated wound segmentation and classification of seven common injuries in forensic medicine.," *Forensic Sci Med Pathol*, vol. 20, no. 2, pp. 443–451, Jun. 2024, doi: 10.1007/s12024-023-00668-5.

[9] H. Carrión, M. Jafari, M. D. Bagood, H. Yang, R. R. Isseroff, and M. Gomez, "Automatic wound detection and size estimation using deep learning algorithms," *PLoS Comput Biol*, vol. 18, no. 3, p. e1009852, Mar. 2022, doi: 10.1371/journal.pcbi.1009852.

[10] L. Dang *et al.*, "Novel Prediction Method Applied to Wound Age Estimation: Developing a Stacking Ensemble Model to Improve Predictive Performance Based on Multi-mRNA," *Diagnostics*, vol. 13, no. 3, p. 395, Jan. 2023, doi: 10.3390/diagnostics13030395.

[11] C. Zhao, Y. Guo, L. Li, and M. Yang, "Non-invasive techniques for wound assessment: A comprehensive review.," *Int Wound J*, vol. 21, no. 11, p. e70109, Nov. 2024, doi: 10.1111/iwj.70109.

[12] D. Griffa *et al.*, "Artificial Intelligence in Wound Care: A Narrative Review of the Currently Available Mobile Apps for Automatic Ulcer Segmentation," Oct. 16, 2024. doi: 10.20944/preprints202410.1244.v1.

[13] B. Zorić, D. Bajer, and M. Dudjak, "Feature extraction procedures for chronic wound tissue classification," in *2024 Zooming Innovation in Consumer Technologies Conference (ZINC)*, May 2024, pp. 1–6. doi: 10.1109/ZINC61849.2024.10579393.

[14] M. A. Khan and M. A. AlGhamdi, "An intelligent and fast system for detection of grape diseases in RGB, grayscale, YCbCr, HSV and L*a*b* color spaces," *Multimedia Tools and Applications*, vol. 83, no. 17, pp. 50381–50399, May 2024, doi: 10.1007/s11042-023-17446-8.

[15] E. Wahyuni, A. Putri, N. Pelu, Firdaus, and I. Wiraagni, "Image Processing-Based Application for Determining Wound Types in Forensic Medical Cases," *Jurnal Nasional Teknik Elektro*, pp. 12–19, Mar. 2024, doi: 10.25077/jnte.v13n1.1148.2024.

[16] I. A. Wiraagni *et al.*, "An Application for Wound Type Determination Based on Image Processing in Forensic Cases," *International Journal of Medical Toxicology & Forensic Medicine*, vol. 14, no. 2, pp. 1–8, 2024, doi: https:/doi.org/10.32598/ijmtfm.v14i2.43899.

[17] A. Anaya-Isaza, L. Mera-Jiménez, and M. Zequera-Diaz, "An overview of deep learning in medical imaging," *Informatics in Medicine Unlocked*, vol. 26, p. 100723, 2021, doi: 10.1016/j.imu.2021.100723.

[18] R. Zhang, D. Tian, D. Xu, W. Qian, and Y. Yao, "A Survey of Wound Image Analysis Using Deep Learning: Classification, Detection, and Segmentation," *IEEE Access*, vol. 10, pp. 1–1, Jan. 2022, doi: 10.1109/ACCESS.2022.3194529.

[19] D. Bora, A. Gupta, and F. Khan, "Comparing the Performance of L*A*B* and HSV Color Spaces with Respect to Color Image Segmentation," Jun. 2015.
[20] F. Ferreira *et al.*, "A Systematic Investigation of Models for Color Image Processing in Wound Size Estimation," *Computers*, vol. 10, no. 4, p. 43, Apr. 2021, doi: 10.3390/computers10040043.
[21] T. Wu, X. Gu, J. Shao, R. Zhou, and Z. Li, "Color image segmentation based on a convex K-means approach," Mar. 17, 2021, *arXiv*: arXiv:2103.09565. doi: 10.48550/arXiv.2103.09565.
[22] S. R. H. Zaidi and S. Sharma, "Pressure Ulcer," *StatPearls Publishing*, 2024, [Online]. Available: https://www.ncbi.nlm.nih.gov/books/NBK553107/
[23] M. Alauthman *et al.*, "Enhancing Small Medical Dataset Classification Performance Using GAN," *Informatics*, vol. 10, no. 1, p. 28, Mar. 2023, doi: 10.3390/informatics10010028.
[24] K. B. Shaik, P. Ganesan, V. Kalist, B. S. Sathish, and J. M. M. Jenitha, "Comparative Study of Skin Color Detection and Segmentation in HSV and YCbCr Color Space," *Procedia Computer Science*, vol. 57, pp. 41–48, 2015, doi: 10.1016/j.procs.2015.07.362.
[25] F. Jaison, V. K. Pandey, and A. Bishnoi, "Developing Support Vector Machines for Accurate Medical Image Analysis," in *2024 International Conference on Optimization Computing and Wireless Communication (ICOCWC)*, Jan. 2024, pp. 1–7. doi: 10.1109/ICOCWC60930.2024.10470551.
[26] N. Panda, "A Review on Logistic Regression in Medical Research," *National Journal of Community Medicine*, vol. 13, pp. 265–270, Apr. 2022, doi: 10.55489/njcm.134202222.
[27] A. Amro, M. Al-Akhras, K. E. Hindi, M. Habib, and B. A. Shawar, "Instance Reduction for Avoiding Overfitting in Decision Trees," *Journal of Intelligent Systems*, vol. 30, no. 1, pp. 438–459, Jan. 2021, doi: 10.1515/jisys-2020-0061.
[28] S. Swaminathan and B. R. Tantri, "Confusion Matrix-Based Performance Evaluation Metrics," *African Journal of Biomedical Research*, vol. 27, pp. 4023–4031, Nov. 2024, doi: 10.53555/AJBR.v27i4S.4345.
[29] S. K and E. B, "Wound Image Analysis Classifier for Efficient Tracking of Wound Healing Status," *Signal & Image Processing : An International Journal*, vol. 5, pp. 15–27, Apr. 2014, doi: 10.5121/sipij.2014.5202.
[30] M. Reiter, R. Donner, G. Langs, and H. Bischof, "Estimation of Face Depth Maps from Color Textures using Canonical Correlation Analysis," vol. 24, pp. 308–312, 2011, doi: 10.1016/j.proeng.2011.11.2647.